Automated detection of calcified plaque using higher-order spectra cumulant technique in computer tomography angiography images

International Journal of Imaging Systems and Technology

Automated detection of calcified plaque using higher-order spectrum cumulant technique in CTA images

Journal:	*International Journal of Imaging Systems and Technology*
Manuscript ID	Draft
Wiley - Manuscript type:	Research Article
Date Submitted by the Author:	n/a
Complete List of Authors:	Acharya U, Rajendra; Ngee Ann Polytechnic Meiburger, Kristen Koh, Joel E. W.; Ngee Ann Polytechnic Ciaccio, Edward Vicnesh, Jahmunah Keow, Tan Sock Wong, Jeannie Azmal, Raja Rizal Hoong, Ng Kwan
Keywords:	Automated detection, CAD, CTA, higher-order spectrum cumulants

Automated detection of calcified plaque using higher-order spectrum cumulant technique in CTA images

U Rajendra Acharya[1,2,3], Kristen M. Meiburger[4], Joel En Wei Koh[1], Edward J Ciaccio[5], Jahmunah Vicnesh[1], Sock Keow Tan[6,7], Jeannie Hsiu Ding Wong[6,7], Raja Rizal Azman Raja Aman[6,7], Kwan Hoong Ng[6,7]

[1]Department of Electronics and Computer Engineering, Ngee Ann Polytechnic, Singapore.

[2]Department of Biomedical Engineering, School of Science and Technology, Singapore University of Social Sciences, Singapore.

[3]School of Medicine, Faculty of Health and Medical Sciences, Taylor's University, Subang Jaya, Malaysia.

[4]Department of Electronics and Telecommunications, Politecnico di Torino, Italy.

[5]Department of Medicine, Columbia University, New York, USA.

[6]Department of Biomedical Imaging, Faculty of Medicine, University of Malaya, 50603 Kuala Lumpur, Malaysia.

[7]University of Malaya Research Imaging Centre (UMRIC), Faculty of Medicine, University of Malaya, 50603 Kuala Lumpur, Malaysia.

Abstract

Cardiovascular diseases continue to be the leading cause of death globally and are often associated with atherosclerosis, which can trigger substantial variations in the coronary arteries, possibly causing coronary artery disease (CAD). Coronary artery calcification is known to be a strong and independent forecaster of CAD. Hence coronary computer tomography angiography (CTA) has become a fundamental non-invasive imaging tool to characterize coronary artery plaques. In this paper, an automated algorithm is presented to uncover the presence of a calcified plaque, using 2060 CTA images acquired from 60 patients. Higher-order spectrum cumulants were extracted from each image, thereby providing 2448 descriptive features per image. The features were then reduced using numerous well-established techniques, and ranked according to t-value. Subsequently, the reduced features were input to several classification methods, to achieve the best diagnostic accuracy with a minimum number of features. Optimal results were obtained using the SVM(Support Vector Machine) with a radial basis function, having 22 features obtained with the Multiple Factor Analysis

feature reduction algorithm. The accuracy, positive predictive value, sensitivity, and specificity obtained were 95.83%, 97.05%, 94.54% and 97.13%, respectively. Based on these results, the technique could be useful to automatically and accurately identify calcified plaque evident in CTA images, and may therefore become an important tool to help reduce procedural costs and patient radiation dose.

1. Introduction

Cardiovascular disease (CVD) is a main factor contributing to mortality worldwide, and it is frequently associated with atherosclerosis, which is brought upon by lipoprotein storage, calcification, muscle cell proliferation, inflammation, necrosis, apoptosis, and fibrosis in the arterial wall [1]. The development of atherosclerosis triggers important variations in the coronary blood vessels, often leading to coronary artery disease (CAD) [1].

In recent years, coronary computer tomography angiography (CTA) has become important for identifying coronary artery stenosis amongst patients suspected to have CAD [2]. Its counterpart, invasive coronary angiography (ICA), has been used as the yardstick for the past decade or so, but it has limitations, including a substantial inter-operator interpretation variability [3]–[5]. Hence, clinical practice and research has been increasingly geared toward the use of the non-invasive CTA technique to express the clinical effect of plaque structure and patient outcome [2]. Moreover, studies have found a link between the amount of coronary artery calcification (CAC) and a robust and independent forecaster of CVD [6]. Typically, to quantify the amount of calcification, two CT scans are required: a calcium scoring CT (CSCT) and a CTA scan, where the CTA scan is used for the detection of non-calcified plaque and stenosis. On the contrary, the amount of calcium is determined by the CSCT scan [7].

In order to decrease the radiation dose during cardiac CT exam, many studies have recently focused on directly using the CTA to quantify calcium, therefore avoiding the CSCT scan [8]–[10]. The manual identification of CAC in cardiac CT is tedious and time-consuming, and numerous studies have been presented in the literature to semi-automatically or automatically calculate calcium from CTA scanning, which typically requires an initial segmentation of the coronary arteries in the imagery. CAC is then either determined as a digression from a trend line

via the lumen strength [11], [12], as voxels that present an intensity beyond a patient-specific Hounsfield Unit (HU) limit within the arteries [13], or as a deviation from a model of non-calcified arterial sections [14]. Recent research in this field has included the implementation of deep learning techniques that automatically segment and quantify calcifications in the coronary arteries [15]–[19]. In particular, Wolterink et al. [16] also provided an assessment of cardiac CT-based automated coronary calcium scoring using 32 training and 40 test exams, where four methods utilized both CSCT and CTA scans, while one only used CSCT. Some of the techniques tested in this study provided satisfying results, showing high sensitivity (Sen), positive predictive value (Ppv),and F1-score (between all methods; for details please refer to the original study [16]) for CAC lesion detection equal to 94%, 96%, and 95%, respectively. However, as stated previously, the majority of these techniques also relied on a CSCT scan. In another study, Wolterink et al. [17] provided a solution for automatic calcium lesion detection that did not rely on a CSCT scan or on coronary artery segmentation, and was based on paired convolutional neural networks. In their study, the authors showed a best sensitivity for lesion identification equal to 72%.

Herein, we propose a novel algorithm for the automatic detection of calcified plaque lesions using only CTA scans, based upon higher order spectrum (HOS) cumulants. The method utilizes image preprocessing, the Radon transform (RT), calculation of HOS cumulants, feature reduction and ranking, and classification. As can be noted, the presented technique does not rely on any segmentation of the coronary arteries within the CTA scan, which would limit applicability in CAC identification, as severe CAC deposits affect the performance of identification methods [20].

2. Materials and Methods

2.1 Image database

The CTA patient scans were performed with a retrospectively ECG-gated protocol, using a 2×32 detector row dual-source CT scanner (Siemens Somatom Definition DS, Siemens Healthcare, Erlangen, Germany) at the University of Malaya Medical Centre, Department of Biomedical Imaging, Malaysia. The analysis of scans acquired from the left anterior descending (LAD) revealed that 30 calcified plaques and 30 normal arteries were present in the 60 patient group (30 female and 30 male, age range: 39 and 81 years, mean value 61.7 ± 9.9 years). For each patient,

a total of 36 true axial views of the proximal LAD (36 mm from bifurcation of LAD and left circumflex (LCx)) were generated at an interval of 1mm from the curved multi-planar reformations (MPR), using a cardiac software package with cutting-edge technology (Syngo.via, Siemens Healthcare, Erlangen, Germany) that is readily available for purchase by the public. (Figure 1). A summary of the image database used in this study is given in Table 1.

2.2 Automatic calcified plaque detection algorithm

Figure 2 displays a step-by-step diagram of the detection algorithm that we propose. Firstly, the image is preprocessed and the Radon transform is computed. Thereafter, the cumulant features are extracted and then reduced using several techniques. Finally, a statistical analysis is done and a classification is obtained using several methods.

2.2.1 Image preprocessing

Examples of the input images to the entire algorithm are shown in Figure 3 (no plaque) and 4 (calcified plaque). The initial step in the calcified plaque detection algorithm is image preprocessing. This step is fundamental to increase the image contrast and to standardize the image pixel intensity distribution. An adaptive histogram equalization algorithm [21] was employed for this operation.

2.2.2 Radon transform (RT)

The RT is typically employed in CT to reconstruct an image from scattering data signals, taking advantage of its mathematical properties, such as symmetry, scaling, linearity, shift, and rotational invariance, in order to discriminate objects [22], [23]. It is also possible to employ the RT to alter 2D images into lines that contain specific parameters given by the projection of the image intensity along a radial line that is oriented at a specific angle. This results in the generation of a line integral which is the summation of the intensities of pixels studied in each direction. Being directional, the RT is thus able to capture directional features, while still preserving pixel intensity variations, which aids in the preservation and boosting of the spatial-frequency information contained in the image. In this work, we computed the RT on every image, with a step size of 10 degrees (i.e., 0°, 10°, 20°, …, 170°), giving forth 17 different 1D RT sonogram signals.

2.2.3 Higher order spectrum (HOS) cumulant feature extraction

Once the RT is applied to the image at every 10° increment, HOS cumulants are then determined for the 1D RT projections. The HOS cumulants are nonlinear combinations of higher-order moments [24]. The benefit of calculating the cumulants is that they are able to capture both the dynamic and nonlinear nature of the input signal. They can be defined as follows.

Let $x(n) = \{x_1, x_2, \ldots, x_k\}$ be the k-dimensional vector of a RT CTA image. The first three moments of $x(n)$, denoted as m_{1_x}, m_{2_x}, and m_{3_x} can be defined as:

$$m_{1_x} = E[x(n)] \quad (1)$$

$$m_{2_x}(\tau_1) = E[x(n)x(n+\tau_1)] \quad (2)$$

$$m_{3_x}(\tau_1, \tau_2) = E[x(n)x(n+\tau_1)x(n+\tau_2)] \quad (3)$$

where $E[\cdot]$ is the statistical expectation operator, and τ_1 and τ_2 are the time lag parameters. Moreover, the first three cumulants of a zero mean process, denoted as c_{1_x}, c_{2_x}, and c_{3_x} can be defined as:

$$c_{1_x} = m_{1_x} \quad (4)$$

$$c_{2_x}(\tau_1) = m_{2_x}(\tau_1) \quad (5)$$

$$c_{3_x}(\tau_1, \tau_2) = m_{3_x}(\tau_1, \tau_2) \quad (6)$$

In the system we present here, we used third-order HOS cumulants of the RT projections. The HOS cumulants that are calculated on each 1D sinogram are described using 136 features; since each image is described with 18 RT sinograms, the total number of features that are used to describe each image is therefore equal to 2448. Figure 5 shows an example of HOS cumulant plots obtained for both a CTA image containing no plaque (first row) and a CTA image containing a calcified plaque (second row).

2.2.4 Feature reduction

Due to the fact that a great number of features are used to represent each image, we tested several data reduction techniques. In particular, we employed the Kernel PCA (KPCA), Locality Preserving Projection (LPP), Locality Sensitive Discriminant Analysis (LSDA), Multiple Factor Analysis (MFA), Principal Component Analysis (PCA) and Neighborhood Preserving Embedding (NPE).

The LPP technique is a linear dimensionality diminution algorithm that is based on the same variational principle that gives rise to the Laplacian Eigenmap, and therefore has similar locality preserving properties [25]. PCA is a common statistical method to extract meaningful features, which is unsupervised and targets to chart the data along the direction having the highest variance [26]. The KPCA method is an extension of PCA, in which the originally linear PCA operations are performed in a reproducing kernel Hilbert space [27]. MFA is an extension PCA that is tailored to identify correlated structure between data sets with matched observations [28]. The main purpose of the LSDA feature reduction technique is to locate a projection which increases the boundary between data from different classes at each local area [26]. The NPE is another reduction algorithm, focusing on preserving local structure [26], [29].

2.2.5 Statistical analysis and classification

Once the features are reduced using various methods as mentioned in the previous subsection, a statistical test is employed to identify highly significant features. In this work, we used Student's t-test, where the features with a higher t-value will represent those that are considered to be significant, while features with a lower t-value will be ranked as less important. Therefore, the reduced features that have the lowest t-values will be considered to best differentiate between images containing no plaque versus those containing a calcified plaque.

The obtained ranked features were then used to enable the completely automatic classification of images containing no plaque and those with a calcified plaque using various classification methods. We used the following well-established techniques for this purpose: decision tree (DT), linear discriminant analysis (LDA), quadratic discriminant analysis (QDA), support vector machine (SVM), k-nearest neighbor (k-NN), and probabilistic neural network (PNN). Also, the SVM classifier with polynomials 1 to 3, coupled with the radial basis function(RBF) were employed. [30]. These classification techniques are explicitly described by Acharya et al. [31].

3. Results

3.1 Feature extraction results

Since each image is described with 2448 features, reduction techniques were incorporated to better compare the results. Table 2 shows the utilized techniques, with the number of significant features which were obtained for each method, as determined by the Student's t-test and ranking. Regarding further detail for each feature reduction method, Table 3 shows the 12 significant features for the KPCA method. Table 4 displays the 12 significant features found using LPP; Table 5 shows the 16 found using the LSDA feature reduction method; Table 6 shows the 22 significant features determined with the MFA technique; Table 7 displays the 14 features found with NPE; finally Table 8 shows the 30 obtained reduced features using PCA. It can be noted from Table 6 that the t-values are higher using MFA than other data reduction techniques. Figure 5 shows the HOS cumulant plots of no plaque and plaque CTA images. These plots show distinctive differences for the two classes.

3.2 Classification results

In this study we employed several well-established classification techniques to process each image as either containing no plaque or containing a calcified plaque. Table 9 summarizes, for each feature reduction technique, which classification method yielded the best results in terms of accuracy, PPV, sensitivity, and specificity. As can be appreciated from the table, that the MFA feature reduction was able to obtain the best classification result among 21 features and a RBF support vector machine classifier. Specifically, a final accuracy of 95.83% was obtained, with a PPV equal to 97.05% and a sensitivity and specificity equal to 94.54% and 97.13%, respectively. To compare classification methods using the MFA feature reduction method, Table 10 shows the results obtained for all of the employed techniques. It can be appreciated that all classification methods provide satisfactory results, many being even higher than the best results obtained using a different feature reduction technique. Figure 6 shows a plot of the first two (MFA8 vs MFA2) MFA coefficients, displaying how even the first two coefficients are capable of exhibiting a distinction between a no plaque image and an image containing a calcified plaque. Hence, we have obtained the highest classification performance using MFA data reduction technique.

4. Discussion and conclusions

In the present study, a database comprising 2060 images from 60 patients was utilized to develop an automated system for detecting the presence of a calcified plaque contained within a CTA scan, and to evaluate the performance of the system. The method is based on the RT, the subsequent calculation of HOS cumulants, and feature reduction and ranking using numerous well-established feature reduction techniques. We showed how, among all of the employed methods, the MFA feature reduction algorithm exhibited by far the best classification results using the SVM coupled with a radial basis function. This algorithm is tailored to identify correlated structure between data sets with matched observations, which proved fundamental in obtaining a high accuracy of 95.83%, when compared to the other feature reduction methods from which was obtained a second-best accuracy equal to 90.23% (LSDA). Moreover, it can be appreciated from Table 9 how, when compared to the second-best performing LSDA technique, the MFA method showed an approximate 3 to 5% increase in both accuracy and sensitivity, and an almost 10% increase when considering PÞv and specificity. This demonstrates how the MFA feature reduction technique, coupled with a SVM and radial basis function, is able to greatly reduce the number of false positives (i.e., images classified as containing calcified plaque that do not really contain it).

As mentioned in the Introduction, the clinical setting is becoming more geared toward the use of non-invasive imaging techniques for the classification and characterization of coronary atherosclerotic plaques, where CTA plays a fundamental role. Since the presence of a calcified plaque has been shown to have an important predictive value for the occurrence of a CVD event, it is of fundamental importance to be able to automatically and accurately detect its presence [6]. Moreover, the use of only one CT scan (i.e., only the CTA scan and not CTA + CSCT scans) presents the advantage of reducing both healthcare costs and the radiation dose a patient must be subject to [32]. Various studies have been previously presented in the literature to confront the issue of automatic detection of calcified plaque in CTA images. However, many of the techniques rely on a first initial segmentation of the coronary artery tree, which can preclude a correct detection in the case of a complex anatomy, during scans with motion or noise artefacts, coronary artery occlusions or distal segments of the vessels [17]. On the other hand, many techniques are also only semi-automatic, requiring an operator to interact with the system to either correct potential errors or to initialize the algorithm [16]. Contrarily, Wolterink et al. [17] presented in 2016 a completely automatic method using only CTA images, based on paired convolutional neural networks for the detection and quantification of CAC, that did not require any initial segmentation. While the method

provided quantitative measurements of a calcium score that showed a good agreement with reference scores, in the best-case scenario it detected only 72% of lesions in the test set (i.e., sensitivity = 72%).

The algorithm that we developed and presented in this study has several advantages:

- A completely automatic classification of calcified plaque without using any segmentation method for the coronary artery tree, or any user-interaction;
- HOS cumulants are able to extract important distinguishable features from the CTA image;
- High performance results: a sensitivity, accuracy and specificity of 94.54%, 95.83%, and 97.13%, respectively, were obtained using an MFA feature reduction method coupled with a SVM with a radial basis function;

There are also some limitations to this work. Firstly, the database only contained information from 60 patients, with either no plaque or a calcified plaque. Therefore, in future work it will be necessary to expand the database to include more patients, and to include images of non-calcified plaques, in order to test its expanded applicability. Furthermore, the proposed method provided a satisfactory sensitivity level for calcified plaque determination, but no quantitative calcium score is calculated. Our future work should include the subsequent implementation of an algorithm for the calculation of a quantitative calcium score on images where a calcified plaque is automatically determined. Deep learning is a part of the artificial intelligence approach that eliminates feature extraction, feature reduction, and categorization, incorporating the entire methodology into one typically convolutional model. In the future, we plan to design a convolutional neural network model with a larger database to not only detect calcified plaque, but also to automatically calculate the calcium score.

In conclusion, this work proposes a novel approach using HOS cumulants, combined with numerous feature reduction techniques, to automatically identify a calcified plaque. The system exhibited promising performance results, and may be developable as a tool for assisting doctors in locating calcified plaques in CTA images.

Acknowledgement

We thank the radiologists and radiographers at the University of Malaya Medical Centre for their kind assistance.

Funding

This study was supported by the High Impact Research Chancellery Grant UM.C/625/1/HIR/MOHE/MED/36 from the Ministry of Education, Malaysia, and the Postgraduate Research Grant PG307-2016A from the University of Malaya, Malaysia.

Conflict of interest:

None

Ethic approval

Medical Ethics Committee of the University of Malaya Medical Centre (Protocol no: 989.35)

References

[1] Agoston-Coldea, L. ,Cionca, C. & Lupu, S.(2005). Coronary CT Angiography and the Napkin-ring Sign Indicates High-Risk Atherosclerotic Lesions. *Intech open*.

[2] Sato, A(2014). Coronary plaque imaging by coronary computed tomography angiography. *World Journal of Radiology*, 6(5), 148.

[3] White, C.W., Wright, C.B., Doty, D.B., Hiratza, L.F., Eastham, C.L., Harrison, D.G., Marcus, M.L.(1984). Does Visual Interpretation of the Coronary Arteriogram Predict the Physiologic Importance of a Coronary Stenosis? *The New England Journal of Medicine*, 310(13), 819–824.

[4] Marcus, M.L., Harrison,D.G.,White, C.W., McPherson, D.D., Wilson,R.F., & Kerber, R.E.(1988). Assessing the physiologic significance of coronary obstructions in patients: Importance of diffuse undetected atherosclerosis. *Progress in Cardiovascular Diseases*, 31(1), 39–56.

[5] Vogel,R.A.(1988). Assessing Stenosis Significance by Coronary Arteriography: Are the Best Variables Good Enough?

[6] Yeboah, J et al (2012). Comparison of Novel Risk Markers for Improvement in Cardiovascular Risk Assessment in Intermediate-Risk Individuals, *Journal of the American Medical Association*, 38(8) , 788-795.

[7] Hecht, H.S.(2015), Coronary Artery Calcium Scanning: Past, Present, and Future, *Journal of*

the Amaerican College of Cardiology: Cardiovascular Imaging, 8(5), 579–596.

[8] Pavitt, C.W et al (2014). Deriving coronary artery calcium scores from CT coronary angiography: a proposed algorithm for evaluating stable chest pain, *The International Journal of Cardiovascular Imaging*, 30(6), 1135–1143.

[9] Messenger, B., Li, D., Nasir,K., Carr, J.J., Blankstein, R., & Budoff, M.J.(2016). Coronary calcium scans and radiation exposure in the multi-ethnic study of atherosclerosis, *International Journal of Cardiovascular Imaging*, 32(3), 525–529.

[10] Al-Mallah, M.H.,Aljizeeri, A., Alharthi, M., & Alsaileek, A.(2014). Routine low-radiation-dose coronary computed tomography angiography, *European Heart Journal Supplements,*16(supplement B), B12–B16.

[11] Wesarg, S., Khan, M.F., & Firle, E.A.(2006). Localizing Calcifications in Cardiac CT Data Sets Using a New Vessel Segmentation Approach, *Journal of Digital Imaging*, 19(3), 249–257.

[12] Ahmed, W et al (2015). Automatic detection and quantification of the Agatston coronary artery calcium score on contrast computed tomography angiography, *International Journal of Cardiovascular Imaging*, 31(1), 151–161.

[13] Teßmann, M., Vega-Higuera, F., Bischoff,B.,Hausleiter, J., & Greiner, G.(2011). Automatic detection and quantification of coronary calcium on 3D CT angiography data, *Computer Science Research and Developemnt,* 26(1-2), 117–124.

[14] Eilot, D. & Goldenberg, R.(2014). Fully automatic model-based calcium segmentation and scoring in coronary CT angiography, *International Journal of Computer Assisted Radiology and Surgery*, 9(4), 595–608.

[15] Zreik, M., van Hamersvelt, R.W., Wolterink, J.M., Leiner, T.,Viergever, M.A., & Isgum, I.(2019). A Recurrent CNN for Automatic Detection and Classification of Coronary Artery Plaque and Stenosis in Coronary CT Angiography, *IEEE Transactionas on Medical Imaging*.

[16] Wolterink, J.M et al (2016). An evaluation of automatic coronary artery calcium scoring methods with cardiac CT using the orCaScore framework," *Medical Physics,* 43(5) 2361–2373.

[17] Wolterink, J.M., Leiner, T., de Vos, B.D., van Hamersvelt, R.W., Viergever, M.A., & Išgum, I.(2016). Automatic coronary artery calcium scoring in cardiac CT angiography using paired convolutional neural networks, *Medical Image Analysis,* 34,123–136.

[18] Lessmann, N et al(2018). Automatic Calcium Scoring in Low-Dose Chest CT Using Deep Neural Networks With Dilated Convolutions, *IEEE Transactions on Medical Imaging*, 37(2), 615–625.

[19] Shadmi, R., Mazo, V., Bregman-Amitai, O., & Elnekave, E.(2018). Fully-convolutional deep-learning based system for coronary calcium score prediction from non-contrast chest CT, *2018 IEEE 15th International Symposium on Biomedical Imaging (ISBI 2018)*, 24-28.

[20] Schaap. M et al (2009). Standardized evaluation methodology and reference database for evaluating coronary artery centerline extraction algorithms," *Medical Image Analysis,* 13(5), 701–714.

[21] Pizer, S.M et al (1987). Adaptive histogram equalization and its variations," *Computer Vision, Graphics and Image Processing,* 39(3),355–368.

[22] Mookiah, M.R.K et al (2015). Application of higher-order spectra for automated grading of diabetic maculopathy," *Medical and Biological Enginering and Computing,* 53(12),1319–1331.

[23] Radon, J.(1986). On the determination of functions from their integral values along certain manifolds, *IEEE Transactionas on Medical Imaging*, 5(4), 170–176.

[24] Noronha, K.P., Acharya, U.R., Nayak, k.P., Martis, R.J., & Bhandary, S.V.(2014). Automated classification of glaucoma stages using higher order cumulant features, *Biomedical Signal Processing Control*, 10(1), 174–183.

[25] He, X., Niyogi, P.(2004) in neural information processing systems, and undefined 2004, Locality preserving projections, *Advances in. Neural Information Processing Systems,* 153–160.

[26] Cai, D., He, X., Zhou, K., Han, J., & Bao, H.(2007). Locality Sensitive Discriminant Analysis in *20th International Joint Conference on Artificial Intelligence*, 708–713.

[27] Schölkopf, B., Smola, A., & Müller, K.R.(1988). Nonlinear Component Analysis as a Kernel Eigenvalue Problem, *Neural Computation,* 10(5), 1299–1319.

[28] Meng, C., Zeleznik, O.A.,Thallinger, G.G., Kuster, B., Gholami, A.M., & Culhane, A.C.(2016). Dimension reduction techniques for the integrative analysis of multi-omics data," *Briefings in Bioinformatics,* 17(4), 628–641.

[29] He, X., Cai, D., Yan, S., & Zhang, H.J(2005). Neighborhood preserving embedding in *Tenth IEEE International Conference on Computer Vision (ICCV'05)*,1, 1208–1213.

[30] Duda, R., Hart, P., & Stork, D.(2012). *Pattern classification*.

[31] U. R. Acharya et al(2016). Automated characterization of fatty liver disease and cirrhosis using curvelet transform and entropy features extracted from ultrasound images, *Computers in Biology and Medicine,* 79, 250–258.

[32] Voros, S., & Qian, Z.(2012). Agatston score tried and true: By contrast, can we quantify calcium on CTA? *Journal of Cardiovascular Computer Tomography*, 16(1),45–47.

Tables and Figures

Table 1. Summary of patient and image database.

Table 2. Summary of feature reduction methods employed.

KPCA: Kernel PCA;
LPP: Locality Preserving Projection;
LSDA: Locality Sensitive Discriminant Analysis;
MFA: Multiple Factor Analysis;
PCA: Principal Component Analysis;
NPE: Neighborhood Preserving Embedding

Table 3. Results obtained after feature reduction using Kernel Principal Component Analysis (KPCA).

Table 4. Results obtained after feature reduction using Locality Preserving Projection (LPP).

Table 5. Results obtained after feature reduction using Locality Sensitive Discriminant Analysis (LSDA).

Table 6. Results obtained after feature reduction using Multiple Factor Analysis (MFA).

Table 7. Results obtained after feature reduction using Neighbourhood Preserving Embedding (NPE).

Table 8. Results obtained after feature reduction using Principal Component Analysis (PCA).

Table 9. Best classification results for calcification plaque determination using different feature reduction techniques.

para: parameters, Aç.: accuracy, PÞv: positive predictive value, Sen: sensitivity, Spe: specificity

Table 10. Results for the classification of calcified plaque detection using Multiple Factor Analysis (MFA) feature reduction.

para: parameters, Aç.: accuracy, PÞv: positive predictive value, Sen: sensitivity, Spe: specificity

Figure 1. Curved multi-planar reformations (MPR) of the left anterior descending (LAD) artery with true axial views generated at an interval of 1mm.

Figure 2. Step-by-step diagram of the calcified plaque detection algorithm.

Figure 3. Example CTA images with no plaque.

Figure 4. Example CTA images with calcified plaque.

Figure 5. Examples of higher order spectrum cumulants. (A) Example no plaque CTA image; (B) Contour plot of no plaque CTA image; (C) 3D contour plot of no plaque CTA image; (D) Example calcified plaque CTA image; (E) Contour plot of calcified plaque CTA image; (F) 3D contour plot of calcified plaque CTA image.

Figure 6. Scatter plot showing first two MFA features of non-calcified plaque in blue, and calcified plaques in red color.

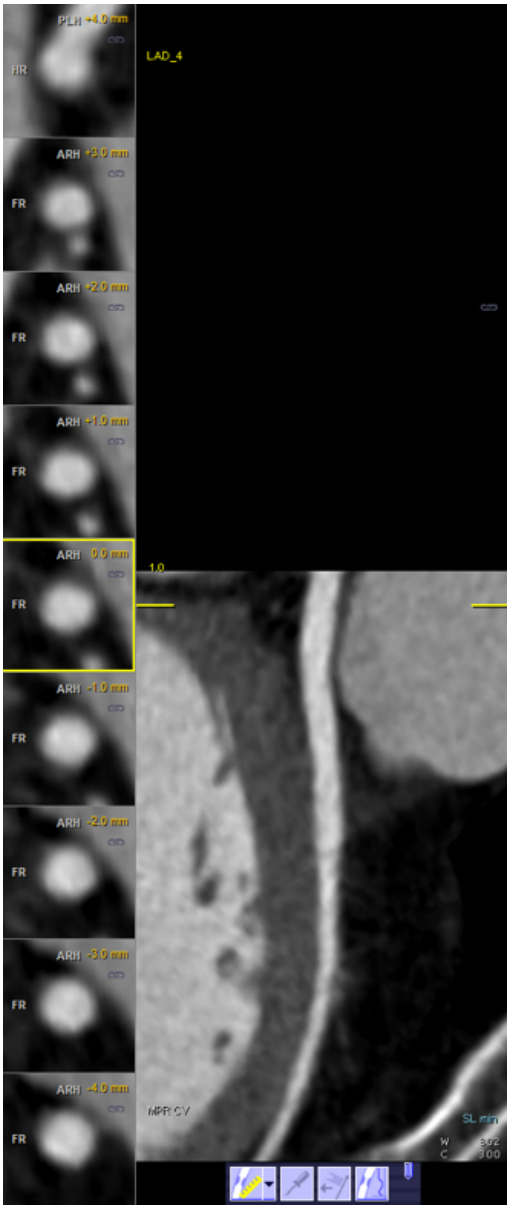

Figure 1. Curved multi-planar reformations (MPR) of the left anterior descending (LAD) artery with true axial views generated at an interval of 1mm.

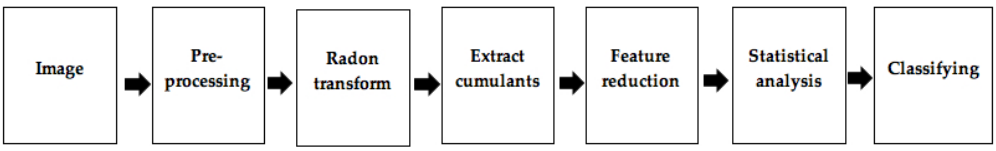

Figure 2. Step-by-step diagram of the calcified plaque detection algorithm.

283x43mm (72 x 72 DPI)

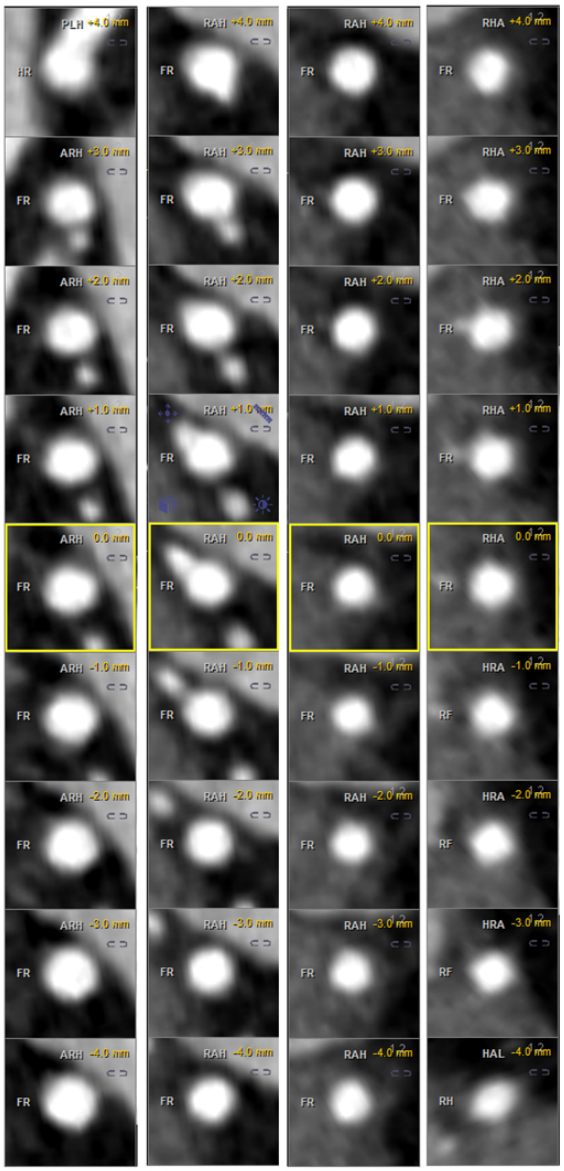

Figure 3. Example CTA images with no plaque.

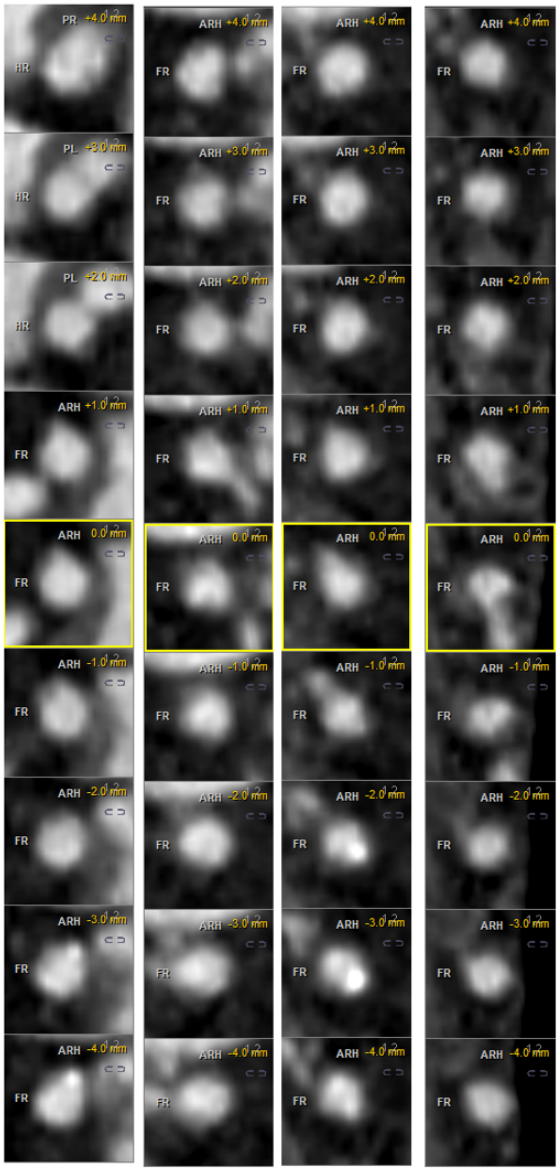

Figure 4. Example CTA images with calcified plaque.

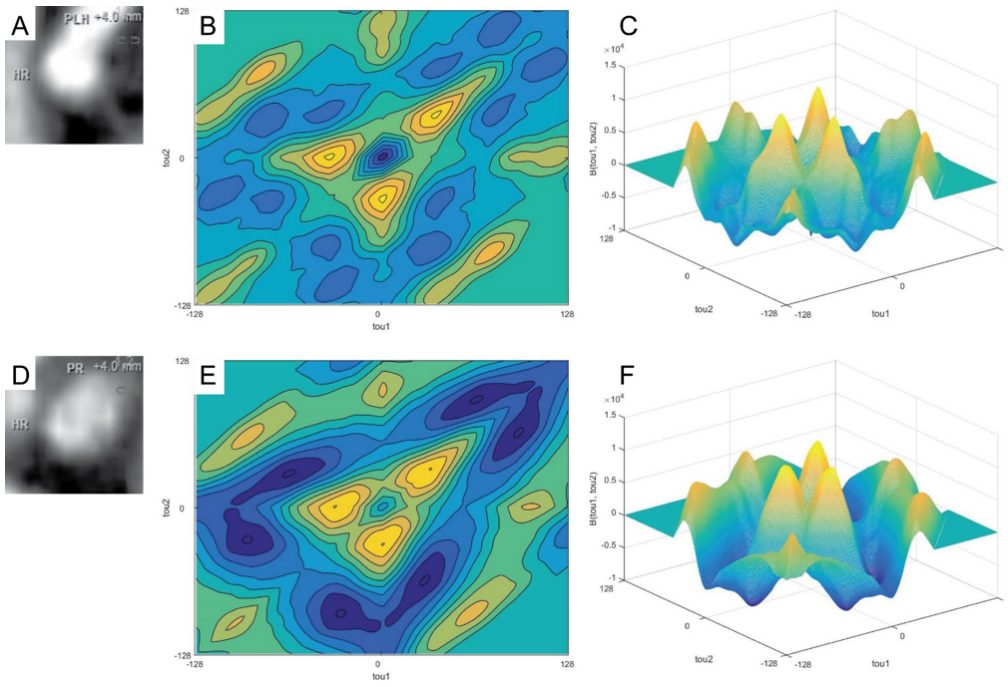

Figure 5. Examples of higher order spectrum cumulants. (A) Example no plaque CTA image; (B) Contour plot of no plaque CTA image; (C) 3D contour plot of no plaque CTA image; (D) Example calcified plaque CTA image; (E) Contour plot of calcified plaque CTA image; (F) 3D contour plot of calcified plaque CTA image.

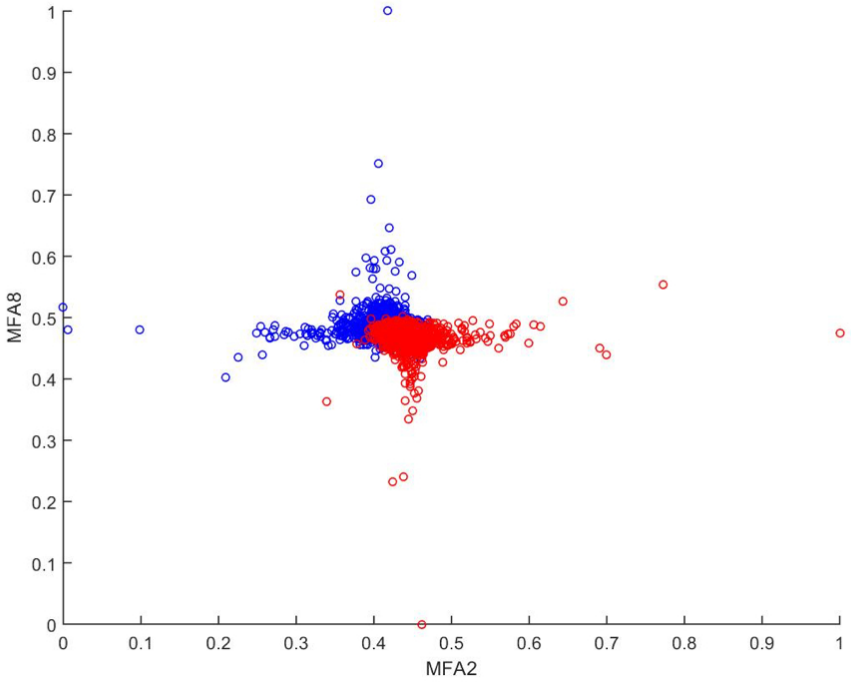

Figure 6. Scatter plot showing first two MFA features of non-calcified plaque in blue, and calcified plaques in red color.

Table 1. Summary of patient and image database.

Class	Number of subjects	Number of images
No plaque	30	1080
Calcified plaque	30	1080

Table 2. Summary of feature reduction methods employed.

Algorithm	Total number of features	Number of significant features
KPCA	30	12
LPP	30	12
LSDA	30	16
MFA	30	22
NPE	30	14
PCA	435	30

Table 3. Results obtained after feature reduction using Kernel Principal Component Analysis (KPCA).

kPCA coefficient	No plaque		Calcified plaque		p-value	t-value
	Mean	SD	Mean	SD		
kPCA12	0.5410	0.0898	0.5145	0.1084	0.0000	6.1853
kPCA23	0.4889	0.1085	0.4692	0.1211	0.0001	3.9873
kPCA17	0.4663	0.0797	0.4786	0.0858	0.0006	3.4562
kPCA28	0.4700	0.0553	0.4781	0.0602	0.0011	3.2768
kPCA7	0.4872	0.0891	0.4741	0.1004	0.0014	3.2052
kPCA5	0.5115	0.0742	0.5210	0.0824	0.0047	2.8294

kPCA4	0.5975	0.0722	0.5885	0.0867	0.0088	2.6227
kPCA29	0.5982	0.1040	0.5867	0.1070	0.0116	2.5274
kPCA3	0.7970	0.0780	0.7889	0.0781	0.0162	2.4067
kPCA11	0.6414	0.0673	0.6486	0.0820	0.0241	2.2571
kPCA21	0.5104	0.0987	0.5200	0.1113	0.0326	2.1379
kPCA15	0.5065	0.0767	0.4995	0.0891	0.0493	1.9673

Table 4. Results obtained after feature reduction using Locality Preserving Projection (LPP).

LPP coefficient	No plaque		Calcified plaque		p-value	t-value
	Mean	SD	Mean	SD		
LPP13	0.3839	0.0748	0.4062	0.0916	0.0000	6.2174
LPP9	0.5786	0.0943	0.5546	0.1100	0.0000	5.4452
LPP26	0.5884	0.0622	0.5714	0.0845	0.0000	5.2979
LPP10	0.6216	0.0572	0.6104	0.0680	0.0000	4.1662
LPP17	0.5067	0.1067	0.4893	0.1045	0.0001	3.8349
LPP18	0.4814	0.0849	0.4673	0.0966	0.0003	3.6030
LPP5	0.4138	0.0647	0.4027	0.0858	0.0007	3.3953
LPP7	0.7195	0.0897	0.7327	0.0901	0.0007	3.3900
LPP12	0.6169	0.0662	0.6272	0.0760	0.0008	3.3626
LPP29	0.3352	0.0802	0.3240	0.0796	0.0012	3.2371
LPP4	0.4125	0.0819	0.4239	0.0988	0.0035	2.9277
LPP21	0.5449	0.1040	0.5582	0.1123	0.0042	2.8665

Table 5. Results obtained after feature reduction using Locality Sensitive Discriminant Analysis (LSDA).

LSDA coefficient	No plaque		Calcified plaque		p-value	t-value
	Mean	SD	Mean	SD		
LSDA9	0.5435	0.0691	0.5039	0.1116	0.0000	9.8969
LSDA6	0.6766	0.0557	0.6467	0.0979	0.0000	8.7180
LSDA11	0.5996	0.1102	0.5607	0.0991	0.0000	8.6189
LSDA8	0.4978	0.0663	0.4723	0.0734	0.0000	8.4847
LSDA4	0.2318	0.0638	0.2602	0.0920	0.0000	8.3225
LSDA14	0.5254	0.1019	0.5603	0.1019	0.0000	7.9602
LSDA21	0.6342	0.0575	0.6137	0.0806	0.0000	6.8070
LSDA12	0.8278	0.0440	0.8132	0.0635	0.0000	6.2001
LSDA20	0.6289	0.0791	0.6486	0.1045	0.0000	4.9544
LSDA17	0.6518	0.0879	0.6326	0.0990	0.0000	4.7539
LSDA15	0.4543	0.0827	0.4382	0.0805	0.0000	4.5812
LSDA26	0.5382	0.0839	0.5546	0.0866	0.0000	4.4499
LSDA3	0.7363	0.1265	0.7162	0.1434	0.0006	3.4536
LSDA16	0.5768	0.1045	0.5617	0.1076	0.0009	3.3103
LSDA7	0.4854	0.0877	0.4727	0.0967	0.0015	3.1847
LSDA19	0.5413	0.0947	0.5297	0.0972	0.0050	2.8075

Table 6. Results obtained after feature reduction using Multiple Factor Analysis (MFA).

MFA coefficient	No plaque		Calcified plaque		p-value	t-value
	Mean	SD	Mean	SD		
MFA2	0.4099	0.0355	0.4449	0.0353	0.0000	22.9956
MFA8	0.4870	0.0267	0.4657	0.0247	0.0000	19.3028
MFA7	0.5206	0.0360	0.4969	0.0345	0.0000	15.6184
MFA5	0.5082	0.0271	0.4933	0.0249	0.0000	13.3261
MFA1	0.3775	0.0250	0.3952	0.0390	0.0000	12.5085
MFA13	0.5304	0.0240	0.5185	0.0240	0.0000	11.5565
MFA10	0.4975	0.0299	0.5092	0.0301	0.0000	9.0257
MFA21	0.4875	0.1504	0.5375	0.1274	0.0000	8.3350
MFA29	0.5333	0.1221	0.5766	0.1259	0.0000	8.1189
MFA3	0.5959	0.0362	0.6074	0.0322	0.0000	7.7910
MFA4	0.3739	0.0273	0.3814	0.0283	0.0000	6.2558
MFA6	0.5222	0.0454	0.5330	0.0426	0.0000	5.7051
MFA11	0.5700	0.0341	0.5623	0.0326	0.0000	5.3125
MFA30	0.4721	0.1434	0.4425	0.1151	0.0000	5.3026
MFA25	0.4751	0.1396	0.5034	0.1213	0.0000	5.0377
MFA18	0.6229	0.0267	0.6187	0.0194	0.0000	4.1465
MFA12	0.5178	0.0220	0.5140	0.0219	0.0000	4.1013
MFA15	0.5490	0.0256	0.5455	0.0232	0.0008	3.3646
MFA16	0.5350	0.0232	0.5332	0.0060	0.0139	2.4624
MFA17	0.4856	0.0243	0.4838	0.0086	0.0224	2.2862

MFA14	0.6589	0.0300	0.6565	0.0217	0.0339	2.1223
MFA26	0.4957	0.1310	0.5069	0.1202	0.0386	2.0701

Table 7. Results obtained after feature reduction using Neighbourhood Preserving Embedding (NPE).

NPE coefficient	No plaque		Calcified plaque		p-value	t-value
	Mean	SD	Mean	SD		
NPE26	0.5328	0.0822	0.5583	0.0963	0.0000	6.6265
NPE18	0.5368	0.0773	0.5535	0.0803	0.0000	4.9382
NPE12	0.5610	0.0679	0.5729	0.0684	0.0001	4.0638
NPE10	0.5757	0.0471	0.5847	0.0636	0.0002	3.7667
NPE23	0.3437	0.0836	0.3570	0.0960	0.0006	3.4230
NPE5	0.4012	0.0671	0.3906	0.0815	0.0009	3.3162
NPE4	0.4548	0.0751	0.4663	0.0890	0.0012	3.2534
NPE22	0.4347	0.0592	0.4250	0.0807	0.0015	3.1851
NPE7	0.2433	0.0486	0.2531	0.0925	0.0020	3.0896
NPE24	0.4185	0.0697	0.4095	0.0653	0.0020	3.0885
NPE3	0.8518	0.0706	0.8419	0.0817	0.0028	2.9954
NPE13	0.4326	0.0366	0.4395	0.0690	0.0037	2.9043
NPE28	0.4938	0.0838	0.5054	0.1038	0.0043	2.8597
NPE14	0.4826	0.0446	0.4776	0.0601	0.0268	2.2156

Table 8. Results obtained after feature reduction using Principal Component Analysis (PCA).

PCA coefficient	No plaque		Calcified plaque		p-value	t-value
	Mean	SD	Mean	SD		
PCA12	0.5410	0.0898	0.5145	0.1084	0.0000	6.1853
PCA68	0.4060	0.0883	0.4301	0.1038	0.0000	5.8140
PCA64	0.4487	0.0927	0.4707	0.1023	0.0000	5.2286
PCA106	0.5132	0.1044	0.4910	0.1111	0.0000	4.7896
PCA237	0.5099	0.1130	0.5330	0.1297	0.0000	4.4080
PCA179	0.5047	0.1103	0.5250	0.1163	0.0000	4.1782
PCA23	0.5111	0.1085	0.5308	0.1211	0.0001	3.9873
PCA107	0.5840	0.0973	0.5662	0.1133	0.0001	3.9165
PCA265	0.4726	0.1070	0.4544	0.1092	0.0001	3.9123
PCA188	0.4768	0.1251	0.4562	0.1332	0.0002	3.7012
PCA327	0.5086	0.1333	0.4866	0.1437	0.0002	3.6884
PCA105	0.5240	0.1037	0.5067	0.1187	0.0003	3.6125
PCA97	0.5268	0.1038	0.5440	0.1181	0.0003	3.5999
PCA17	0.4663	0.0797	0.4786	0.0858	0.0006	3.4562
PCA28	0.4700	0.0553	0.4781	0.0602	0.0011	3.2768
PCA7	0.5128	0.0891	0.5259	0.1004	0.0014	3.2052
PCA341	0.5262	0.0911	0.5131	0.1000	0.0014	3.1984
PCA180	0.3736	0.0805	0.3848	0.0831	0.0015	3.1825
PCA331	0.4798	0.1102	0.4955	0.1191	0.0015	3.1752
PCA45	0.4313	0.0850	0.4434	0.0943	0.0018	3.1290
PCA35	0.6098	0.1011	0.5963	0.1036	0.0022	3.0627

PCA65	0.5923	0.0761	0.5812	0.0934	0.0026	3.0176
PCA171	0.5152	0.1008	0.5016	0.1089	0.0026	3.0158
PCA242	0.6059	0.1132	0.6207	0.1184	0.0030	2.9687
PCA135	0.5400	0.1038	0.5266	0.1083	0.0036	2.9181
PCA170	0.3969	0.1013	0.4095	0.1017	0.0038	2.8989
PCA221	0.5377	0.1043	0.5240	0.1181	0.0046	2.8387
PCA292	0.5316	0.1320	0.5152	0.1371	0.0046	2.8335
PCA5	0.5115	0.0742	0.5210	0.0824	0.0047	2.8294
PCA44	0.4916	0.1122	0.4777	0.1168	0.0050	2.8110

Table 9. Best classification results for calcification plaque determination using different feature reduction techniques.

Feature reduction technique	Classifier	No. of para.	Aç. (%)	PÞv. %)	Sen. (%)	Spe. (%)
KPCA	PNN	12	71.62	75.19	64.54	78.70
LPP	PNN	19	76.76	76.04	78.15	75.37
LSDA	PNN	21	90.23	89.04	91.76	88.70
MFA	**SVM RBF**	**21**	**95.83**	**97.05**	**94.54**	**97.13**
NPE	PNN	14	74.86	75.69	73.24	76.48
PCA	SVM Poly 3	79	80.56	81.13	79.63	81.48

para: parameters, Aç.: accuracy, PÞv: positive predictive value, Sen: sensitivity, Spe: specificity

Table 10. Results for the classification of calcified plaque detection using Multiple Factor Analysis (MFA) feature reduction.

Classifier	No. of para.	Aç. (%)	PÞv. (%)	Sen. (%)	Spe. (%)
DT	15	86.53	86.56	86.48	86.57
LDA	16	90.09	89.87	90.37	89.81
QDA	15	89.40	89.51	89.26	89.54
SVM Poly 1	19	90.42	90.91	89.81	91.02
SVM Poly 2	17	92.64	92.84	92.41	92.87
SVM Poly 3	11	89.35	88.71	90.19	88.52
k-NN	7	91.39	90.64	92.31	90.46
PNN	7	91.53	90.66	92.59	90.46
SVM RBF	**21**	**95.83**	**97.05**	**94.54**	**97.13**

para: parameters, Aç.: accuracy, PÞv: positive predictive value, Sen: sensitivity, Spe: specificity